

# Near-Infrared Fourier Transform Raman Spectroscopy of B<sub>12</sub> Models. 4. Steric and Electronic Factors Affecting the Co–C Bond in Organocobalt Complexes

Manu Chopra,<sup>†,‡</sup> Tom S. M. Hun,<sup>†</sup> Wa-Hung Leung,<sup>\*,†</sup> and Nai-Teng Yu<sup>\*,†</sup>

Department of Chemistry, The Hong Kong University of Science and Technology, Clear Water Bay, Kowloon, Hong Kong, and School of Chemistry and Biochemistry, Georgia Institute of Technology, Atlanta, Georgia

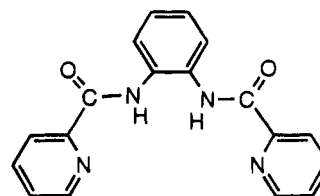
Received April 26, 1995<sup>®</sup>

Cobalt(III)  $\sigma$ -alkyls [Co(bpb)R(OH<sub>2</sub>)] [bpb = 1,2-bis(2-pyridinecarboxamido)benzene; R = CH<sub>3</sub>, C<sub>2</sub>H<sub>5</sub>, *i*-Pr, *n*-Bu, Bz, Np, CH<sub>2</sub>SiMe<sub>3</sub>] were prepared by reactions of Na[Co(bpb)] with the respective alkyl halides. Oxidation of [Co(bpb)CH<sub>3</sub>(OH<sub>2</sub>)] with Ce(IV) gave [Co(bpb)CH<sub>3</sub>]<sup>+</sup>, which shows an isotropic EPR signal at  $g = 2.0800$  with <sup>59</sup>Co hyperfine coupling of ca. 50 G, indicative of Co(IV) character. Treatment of [Co(bpb)CH<sub>3</sub>]<sup>+</sup> with *t*-Bupy (4-*tert*-butylpyridine) led to Co–C bond cleavage and formation of [Co(bpb)(*t*-Bupy)]<sup>+</sup>. The Co–C stretching frequencies for [Co(bpb)CH<sub>3</sub>(OH<sub>2</sub>)] and [Co(bpb)(CN)<sub>2</sub>]<sup>–</sup> have been determined by near-IR FT-Raman spectroscopy to be respectively 515 and 493 cm<sup>–1</sup>, the assignment of which has been confirmed by isotopic labeling experiments. Coordination of bases such as PMe<sub>3</sub> and *t*-Bupy to [Co(bpb)CH<sub>3</sub>(OH<sub>2</sub>)] decreases the Co–C stretching frequency. Treatment of [Co(bpb)CH<sub>3</sub>(OH<sub>2</sub>)] with Ce(IV) results in a downshift of  $\nu(\text{Co–C})$  by 24 cm<sup>–1</sup>, suggesting that the Co–C bond is weakened on oxidation. The Co–C vibrational modes for the heavier alkyls [Co(bpb)R(OH<sub>2</sub>)] (R = C<sub>2</sub>H<sub>5</sub>, *i*-Pr, *n*-Bu, Bz, Np, CH<sub>2</sub>SiMe<sub>3</sub>) have been unambiguously determined to be 483, 478, 400, 334, 307, and 270 cm<sup>–1</sup>, respectively. The  $\nu(\text{Co–C})$  modes for methylcobalt(III) porphyrins [Co(TPP)CH<sub>3</sub>], [Co(OEP)CH<sub>3</sub>], and [Co(TMP)CH<sub>3</sub>]<sup>§</sup> were determined to be 504, 500, and 459 cm<sup>–1</sup>, respectively, indicating that the steric bulk of the porphyrin macrocycle has a profound influence on the axial Co–C bond.

## Introduction

The study of ( $\sigma$ -organo)cobalt(III) compounds is of interest because of its relevance to the biochemistry of the B<sub>12</sub> coenzymes.<sup>1,2</sup> It is generally believed that the key step of the B<sub>12</sub>-dependent rearrangements involves homolytic cleavage of cobalt–carbon bond, which is triggered by structural distortions in the floppy corrin ring of the enzyme.<sup>2,3</sup> However, the exact nature of the conformational changes that induce Co–C bond scission is unclear. An understanding of the factors affecting the cobalt–carbon bond dissociation energy (BDE) in organocobalt compounds will help shed light on the mechanism of B<sub>12</sub>-dependent reactions. Factors that might affect the Co–C BDE of B<sub>12</sub> model compounds of the type [Co(L)R(B)] (L = macrocyclic ligand, B = axial ligand) include the nature of axial bases, oxidation state of Co, the stereoelectronic properties of macrocyclic ligands, and the steric bulk of the R group. Halpern et al.<sup>4</sup> explained the trans electronic effect of axial ligands on the Co–C BDE in terms of the stabilization of the Co(III) over the Co(II) state. In this respect, the trans electronic effect on

the Co–C bond should be treated as a product and/or ground state effect. We have identified the Co–C stretching frequencies of photolabile methylcobalamin and -cobaloxime by near-IR Fourier transform (FT) Raman spectroscopy.<sup>5</sup> The attractiveness of the FT-Raman techniques in providing vibrational information on organocobalt compounds in both solution and the solid state has been pointed out in a previous paper.<sup>5c</sup> Importantly, the Co–C stretching frequency could be correlated with the Co–C bond length, as well as the ground state Co–C BDE of organocobalt compounds. In the study of [Co(DH)<sub>2</sub>CH<sub>3</sub>(Xpy)] (DH = monoanion of dimethylglyoxime, Xpy = para-substituted pyridine), we found that the electronic properties of axial Xpy have little influence on  $\nu(\text{Co–C})$ .<sup>5c</sup> To further elucidate the stereoelectronic factors governing the Co–C bond strength of organocobalt compounds, we set out to study the Raman spectra of cobalt alkyls other than methyl. The identification of Co–C vibrational modes for Co complexes of bulky alkyls such as neopentyl may help predict the  $\nu(\text{Co–C})$  for the B<sub>12</sub> coenzymes, given the comparable steric demands of the neopentyl and adenosyl groups.<sup>6,7</sup> Moreover homolysis of the Co–C bond of organocobalt complexes is also known to be dependent on the oxidation state of Co. The rate of Co–C cleavage in alkylcobalamins is found to be greatly enhanced by electron transfer.<sup>8</sup> Recently, Che and co-workers synthesized some light- and air-stable Co(III) alkyls of a tetradentate dianionic pyridine–amido ligand (bpb), which can undergo reversible one-electron



H<sub>2</sub>(bpb)

\* Authors to whom correspondence should be addressed.

<sup>†</sup> The Hong Kong University of Science and Technology.

<sup>‡</sup> Georgia Institute of Technology.

<sup>§</sup> Abbreviations: *i*-Pr = isopropyl, *n*-Bu = *n*-butyl, Bz = benzyl, Np = neopentyl; H<sub>2</sub>OEP = octaethylporphyrin, H<sub>2</sub>TPP = *meso*-tetraphenylporphyrin, H<sub>2</sub>TMP = *meso*-tetramesitylporphyrin.

<sup>®</sup> Abstract published in *Advance ACS Abstracts*, October 15, 1995.

(1) B<sub>12</sub>: Dolphin, D., Ed.; Wiley: New York, 1982.

(2) Halpern, J. *Science* **1985**, *227*, 869.

(3) (a) Randaccio, L.; Bresciani-Pahor, N.; Zangrando, E.; Marzilli, L. G. *Chem. Soc. Rev.* **1985**, *18*, 225. (b) Toscano, P. J.; Marzilli, L. G. *Prog. Inorg. Chem.* **1984**, *31*, 105. (c) Finke, R. G.; Schiraldi, D. A.; Mayer, B. J. *Coord. Chem. Rev.* **1984**, *54*, 1. (d) Marzilli, L. G. In *Bioinorganic Catalysis*; Reedijk, J., Ed.; Dekker: New York, 1992; Chapter 8, p 227.

(4) (a) Halpern, J.; Ng, F. T. T.; Rempel, G. L. *J. Am. Chem. Soc.* **1979**, *101*, 7124. (b) Ng, F. T. T.; Rempel, G. L.; Halpern, J. *J. Am. Chem. Soc.* **1982**, *104*, 621. (c) Tsou, T.-T.; Loots, M.; Halpern, J. *J. Am. Chem. Soc.* **1982**, *104*, 623.

oxidation.<sup>9</sup> Stable bulky alkyls of Co(bpb) could be prepared readily and may serve as convenient models for cobalamins. Additionally, the Raman study of [Co(bpb)R(OH<sub>2</sub>)]<sup>+</sup> offers a unique opportunity to probe the dependence of axial Co—C bond strength on the oxidation state of Co. The study of [Co(por)R] (por = porphyrinato dianion) as B<sub>12</sub> models is also of significance because of the structural similarity between porphyrin and corrin rings. Furthermore the steric bulk of synthetic *meso*-tetraarylporphyrin can be “tuned” easily by changing the substituent of the *meso* phenyl rings. This allows us to investigate the steric effect of the porphyrin macrocycle on the axial Co—C bond of [Co(por)R].

## Experimental Section

All solvents were purified by standard procedures and distilled prior to use. UV–visible spectra were obtained on a Milton Roy Spectronic 3000 diode array spectrophotometer, and infrared spectra (Nujol) on a Nicolet MAGNA-IR 800 FT-IR spectrophotometer. NMR spectra (in CD<sub>3</sub>OD, unless otherwise stated) were obtained on a JEOL EX400 spectrometer. The EPR spectrum was recorded on a Varian E12 (X-band) spectrometer. Cyclic voltammetry was performed with a Princeton Applied Research (PAR) Model 273A potentiostat. Potentials were determined with respect to a Ag<sup>+</sup>–Ag reference electrode in acetonitrile but are reported with respect to the ferrocenium–ferrocene couple as measured in the same solution.

**Materials.** CD<sub>3</sub>I, C<sub>2</sub>D<sub>5</sub>I, *i*-PrBr-*d*<sub>7</sub>, BzCl-*d*<sub>7</sub>, K<sup>13</sup>CN, KC<sup>15</sup>N, K<sup>13</sup>C<sup>15</sup>N, and H<sub>2</sub>OEP were obtained from Aldrich and used as received. [Co(bpb)(OH<sub>2</sub>)], Na[Co(bpb)(CN)<sub>2</sub>], [Co(bpb)R(OH<sub>2</sub>)] (R = CH<sub>3</sub>, C<sub>2</sub>H<sub>5</sub>, *i*-Pr)<sup>9</sup> H<sub>2</sub>TPP,<sup>10</sup> H<sub>2</sub>TMP,<sup>11</sup> and Co(por)R<sup>12</sup> [por = TPP (*meso*-tetraphenylporphyrin), OEP (octaethylporphyrin), TMP (*meso*-tetramesitylporphyrin); R = CH<sub>3</sub>, CD<sub>3</sub>] were prepared according to the literature methods.

**Syntheses of [Co(bpb)R(OH<sub>2</sub>)] [R = CD<sub>3</sub> (1), C<sub>2</sub>D<sub>5</sub> (2), *i*-Pr-*d*<sub>7</sub> (3), *n*-Bu (4), Bz (5), Bz-*d*<sub>7</sub> (6), CH<sub>2</sub>SiMe<sub>3</sub> (7), Np (8)].** These complexes were prepared according to the literature method<sup>9</sup> from [Co(bpb)(OH<sub>2</sub>)] and RX (X = I for 1, 2; Br for 3, 4, 7, 8; Cl for 5, 6). Typically, to a solution of [Co(bpb)(OH<sub>2</sub>)] (0.1 g) and NaOH (0.1 g) in CH<sub>3</sub>OH (10 mL) was added NaBH<sub>4</sub> (50 mg), and the resulting mixture was stirred at room temperature under nitrogen for 0.5 h, during which a dark green solid precipitated. To this suspension was added excess RX (0.5 mL) and the green solid redissolved to give a dark red solution. The mixture was stirred for 15 min and evaporated to 5 mL, and 100 mL of water was added. The dark red solid was collected and redissolved in acetonitrile. The product was purified by column chromatography (neutral alumina), eluted by CH<sub>3</sub>OH/CH<sub>3</sub>CN (1:4), and recrystallized from CH<sub>3</sub>OH/Et<sub>2</sub>O (yield 50–70%).

**Syntheses of [Co(bpb)CH<sub>3</sub>(B)] [B = *t*-Bupy (9), PMe<sub>3</sub> (10)].** To a solution of [Co(bpb)CH<sub>3</sub>(OH<sub>2</sub>)] (50 mg) in methanol (10 mL) was added excess L (0.1 mL), and the mixture was stirred at room temperature for 30 min. The volatiles were removed in vacuo, and the residue was washed with Et<sub>2</sub>O. Recrystallization of the residue from CH<sub>2</sub>Cl<sub>2</sub>/hexane afforded orange crystals, which were collected and washed with Et<sub>2</sub>O (yield 50–60%).

**Syntheses of [n-Bu<sub>4</sub>N][Co(bpb)X<sub>2</sub>] [X = CN (11), <sup>13</sup>CN (12), C<sup>15</sup>N (13), <sup>13</sup>C<sup>15</sup>N (14)].** To a solution of [Co(bpb)(OH<sub>2</sub>)] (50 mg) in CH<sub>3</sub>–

OH (25 mL) was added excess KX (25 mg), and the mixture was heated at 50 °C for 1 h. The solvent was removed in vacuo and the residue was redissolved in water. On addition of [n-Bu<sub>4</sub>N]Cl (50 mg), a copious amount of orange solid was formed. The orange precipitate was collected, washed with water, and recrystallized from acetone/Et<sub>2</sub>O to give red crystals (yield 70–80%).

**Synthesis of [Co(bpb)CH<sub>3</sub>](OTf) (OTf = Triflate) (15).** To a methanolic solution of [Co(bpb)CH<sub>3</sub>(OH<sub>2</sub>)] (0.1 g) was added 1.2 equiv of Ag(OTf) (50 mg) at room temperature. The reaction was monitored by UV–vis spectroscopy. The completion of the reaction was indicated by the appearance of an absorption around 600–800 nm. The solvent was removed in vacuo, and the residue was extracted with CH<sub>2</sub>Cl<sub>2</sub>. Careful addition of Et<sub>2</sub>O to the extract and cooling at 0 °C gave brown microcrystals, which were collected and washed with a small amount of Et<sub>2</sub>O. Despite several attempts, we have not been able to obtain correct analytical results for the compound.

**Reaction of [Co(bpb)CH<sub>3</sub>]<sup>+</sup> with *t*-Bupy.** A methanolic solution of [Co(bpb)CH<sub>3</sub>]<sup>+</sup> was prepared *in situ* from [Co(bpb)CH<sub>3</sub>(OH<sub>2</sub>)] (50 mg) and 1 equiv of Ag(OTf) (25 mg). To this solution was added *t*-Bupy (0.1 mL), and the mixture was stirred overnight. The solvent was pumped off, and the residue was washed with ether to give a solid which was characterized as [Co(bpb)(*t*-Bupy)]<sup>+</sup> by <sup>1</sup>H-NMR spectroscopy.

**FT-Raman Spectroscopy.** FT-Raman data were acquired on a Bruker IFS 66 / FRA 106 FT-Raman spectrophotometer (Bruker Analytische Messtechnik GmbH, Karlsruhe, Germany) equipped with a highly sensitive, liquid nitrogen cooled Ge detector. FT-Raman spectra were recorded via 180° scattering. The laser excitation wavelength used was 1.064 μm provided by a CW diode laser-pumped Nd:YAG laser. The number of scans taken for all [Co(bpb)R(L)] compounds was 1000, except for [Co(bpb)Bz(OH<sub>2</sub>)], where 3000 scans were Co-added. The laser power employed was 150–200 mW (defocused). The samples were exposed to the laser beam in the solid form in aluminum sample holders which had a 2-mm hole drilled at the center and the interior surface of the hole was polished. The oxidation of [Co(bpb)CH<sub>3</sub>(OH<sub>2</sub>)] by Ce(IV) in methanol was carried out in a quartz cuvette and monitored by Raman spectroscopy. Aliquots were taken periodically from the reaction mixture, and optical spectra were recorded to ensure that [Co(bpb)CH<sub>3</sub>]<sup>+</sup> did not decompose.

## Results

**Syntheses of Co(bpb)R(L).** The cobalt(III) alkyls [Co(bpb)R(OH<sub>2</sub>)] (R = CD<sub>3</sub>, C<sub>2</sub>D<sub>5</sub>, *i*-Pr-*d*<sub>7</sub>, *n*-Bu, Bz, Bz-*d*<sub>7</sub>, Np, CH<sub>2</sub>SiMe<sub>3</sub>) were prepared by reactions of Na[Co(bpb)] with the respective alkyl halides according to the literature procedures.<sup>9</sup> All these complexes are air and light stable in the solid state but become light sensitive in solution for those with bulky alkyls (e.g., the methyl is indefinitely stable but the isopropyl decomposes in a matter of minutes in the presence of fluorescent light). The axial aqua ligand of these complexes is quite labile and can be easily substituted by bases such as phosphine and pyridine to form adducts that are markedly more reactive than [Co(bpb)R(OH<sub>2</sub>)] (*vide infra*).

As previously reported by Che et al.,<sup>9</sup> [Co(bpb)R(OH<sub>2</sub>)] undergoes reversible one-electron oxidation. However, the assignment of oxidation state for the oxidized species is ambiguous due to the noninnocent nature of bpb. Addition of an equimolar amount of Ag(I) or Ce(IV) to a methanolic solution of [Co(bpb)CH<sub>3</sub>(OH<sub>2</sub>)] (Figure 1) generated the same [Co(bpb)CH<sub>3</sub>]<sup>+</sup> which was obtained by controlled-potential electrolysis.<sup>9</sup> The 77 K EPR spectrum of this species (Figure 2) displays a signal at *g* = 2.0800 with characteristic eight-line pattern due to hyperfine coupling of Co (*I* = 7/2), indicative of Co(IV) character. A similar EPR spectrum has been found for [Co(DH)<sub>2</sub>R]<sup>+</sup> (DH = monoanion of dimethylglyoxime) in which

- (5) (a) Nie, S.; Marzilli, L. G.; Yu, N. T. *J. Am. Chem. Soc.* **1989**, *111*, 9526. (b) Nie, S.; Marzilli P. A.; Marzilli, L. G.; Yu, N. T. *J. Chem. Soc., Chem. Commun.* **1990**, 770. (c) Nie, S.; Marzilli P. A.; Marzilli, L. G.; Yu, N. T. *J. Am. Chem. Soc.* **1990**, *112*, 6084.
- (6) Chemaly, S. M.; Pratt, J. M. *J. Chem. Soc., Dalton Trans.* **1980**, 2274.
- (7) (a) Brown, K. L.; Evans, D. R. *Inorg. Chem.* **1994**, *33*, 525. (b) Calafat, A. M.; Marzilli, L. G. *J. Am. Chem. Soc.* **1993**, *115*, 9182.
- (8) (a) Martin, B. D.; Finke, R. G. *J. Am. Chem. Soc.* **1990**, *112*, 2419. (b) Martin, B. D.; Finke, R. G. *J. Am. Chem. Soc.* **1992**, *114*, 585.
- (9) Mak, S.-T.; Yam, V. W. W.; Che, C.-M.; Wong, W.-T.; Lai, T.-F. *J. Chem. Soc., Dalton Trans.* **1991**, 1915.
- (10) Alder, A. D.; Longo, F. R.; Finarelli, J. D.; Goldmacher, J.; Assour, J.; Korsagoff, L. *J. Org. Chem.* **1967**, *32*, 467.
- (11) Wagner, R. W.; Lawrence, D. S.; Lindsey, J. S. *Tetrahedron Lett.* **1987**, 28, 3069.
- (12) Ogoshi, E.; Watanabe, E.; Koketzu, N.; Yoshida, Z. *Bull. Chem. Soc. Jpn.* **1976**, *49*, 2529.

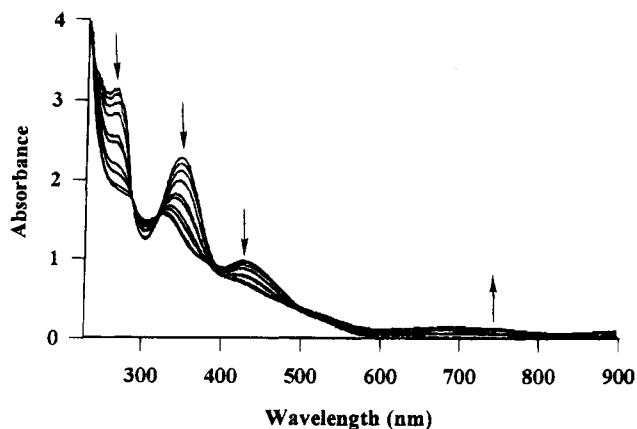


Figure 1. Spectral trace for oxidation of  $[\text{Co}(\text{bpb})\text{CH}_3(\text{OH}_2)]$  by  $\text{Ce}(\text{IV})$  in methanol.

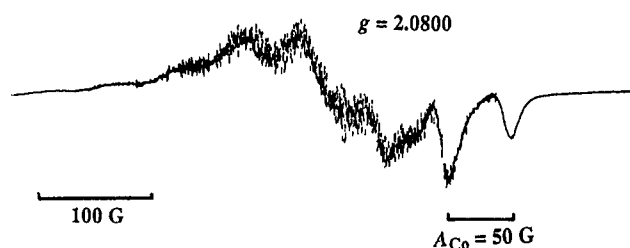
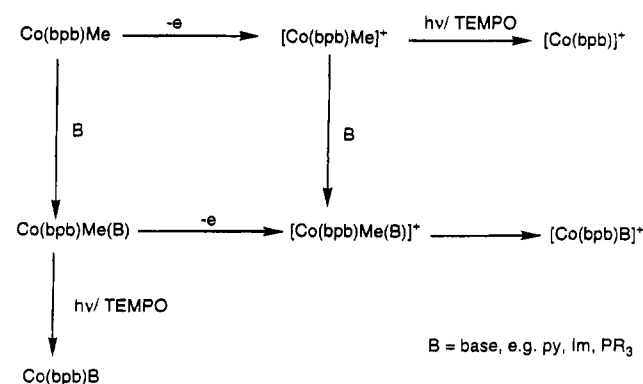


Figure 2. EPR spectrum of  $[\text{Co}(\text{bpb})\text{CH}_3]^+$  in methanol at 77 K. Microwave frequency is 9.205 GHz.

the oxidation state was assigned as IV.<sup>13</sup> We therefore formulate the oxidized species as a Co(IV) compound  $[\text{Co}^{\text{IV}}(\text{bpb})\text{CH}_3]^+$ , which can also have some ligand-centered radical character. The characteristic absorption for this species in the 600–800 nm region, which is absent for both  $[\text{Co}(\text{bpb})(\text{OH}_2)]$  and  $[\text{Co}(\text{bpb})\text{R}(\text{OH}_2)]$ , is tentatively assigned to the amide-to-Co(IV) charge-transfer transition by comparison with the optical spectrum of an analogous Co(IV) phenoxo–amido complex.<sup>14</sup>

$[\text{Co}(\text{bpb})\text{CH}_3]^+$  is stable in solution in the absence of light at room temperature for brief period (12 h) and could be isolated as a brown solid on precipitation with ether. The optical spectrum of this solid is identical to Figure 1, indicating that it was not reduced during the precipitation. However, in the presence of light,  $[\text{Co}(\text{bpb})\text{CH}_3]^+$  decomposes rapidly (in ca. 5 min) in solution, as evidenced by its optical spectrum. Reaction of base (B) such as pyridine with  $[\text{Co}(\text{bpb})\text{CH}_3]^+$  in the dark also resulted in Co–C bond cleavage and formation of  $[\text{Co}(\text{bpb})\text{B}]^+$ , characterized by NMR spectroscopy. We have not been able to detect the pyridinium product, which was observed in the base-induced decomposition Co(IV) cobaloxime and Schiff base analogs.<sup>13,15</sup> However,  $\text{CH}_3$ -TEMPO (TEMPO = 2,2,6,6-tetramethylpiperidinyloxy) was detected for the reaction of  $[\text{Co}(\text{bpb})\text{CH}_3]^+$  with TEMPO. It should be noted that no reaction between  $[\text{Co}(\text{bpb})\text{CH}_3(\text{OH}_2)]$  and TEMPO was observed under the same experimental conditions. Oxidation of the adducts  $[\text{Co}(\text{bpb})\text{CH}_3(\text{B})]$  (B = *t*-Bupy,  $\text{PMe}_3$ ) by  $\text{Ce}(\text{IV})$  gave very reactive Co(IV) species  $[\text{Co}(\text{bpb})\text{CH}_3(\text{B})]^+$ , which decompose rapidly in solution even in the dark to give  $[\text{Co}(\text{bpb})\text{B}]^+$ . The reactivities of  $[\text{Co}(\text{bpb})\text{CH}_3(\text{OH}_2)]$  and  $[\text{Co}(\text{bpb})\text{CH}_3]^+$  are summarized in Scheme 1.

Scheme 1



B = base, e.g. py, Im,  $\text{PR}_3$

Table 1. Oxidation Potentials for  $[\text{Co}(\text{bpb})\text{R}(\text{L})]$  ( $E^\circ$ )<sup>a</sup>

R	L	solvent	$E^\circ[\text{Co}(\text{III/IV})]$ (V vs $\text{Cp}_2\text{Fe}^{+/0}$ )
$\text{CH}_3^b$	$\text{OH}_2$	$\text{CH}_3\text{CN}$	0.22
$\text{CH}_3^b$	$\text{OH}_2$	$\text{CH}_3\text{OH}$	0.31
$\text{CH}_3$	$\text{PMe}_3$	$\text{CH}_3\text{CN}$	0.16 <sup>c</sup>
$\text{CH}_3$	$\text{PMe}_3$	$\text{CH}_3\text{OH}$	0.30 <sup>c</sup>
$\text{Et}^b$	$\text{OH}_2$	$\text{CH}_3\text{CN}$	0.18
<i>i</i> -Pr <sup>b</sup>	$\text{OH}_2$	$\text{CH}_3\text{CN}$	0.19 <sup>c</sup>
<i>n</i> -Bu	$\text{OH}_2$	$\text{CH}_3\text{CN}$	0.18
Np	$\text{OH}_2$	$\text{CH}_3\text{OH}$	0.21
$\text{CH}_2\text{SiMe}_3$	$\text{OH}_2$	$\text{CH}_3\text{OH}$	0.31

<sup>a</sup> Potentials measured at a glassy carbon electrode with 0.1 M  $[n\text{-Bu}_4\text{N}]\text{PF}_6$  as supporting electrolyte. Scan rate = 100 mV s<sup>-1</sup>.

<sup>b</sup> Reference 9. <sup>c</sup> Irreversible.

Table 2. Raman Spectral Data ( $\text{cm}^{-1}$ ) for  $[\text{Co}(\text{bpb})\text{X}(\text{L})]$  in the Solid State

X	L	$\nu(\text{Co}-\text{C})$	$\delta(\text{Co}-\text{C}-\text{N})$	$\nu(\text{C}\equiv\text{N})$
$\text{CH}_3$	$\text{OH}_2$	515		
$\text{CH}_3$	$\text{PMe}_3$	500		
$\text{CH}_3$	<i>t</i> -Bupy	511		
$\text{CD}_3$	$\text{OH}_2$	483		
$\text{C}_2\text{H}_5$	$\text{OH}_2$	488		
$\text{C}_2\text{D}_5$	$\text{OH}_2$	449		
<i>i</i> -Pr	$\text{OH}_2$	478		
<i>i</i> -Pr- $d_7$	$\text{OH}_2$	397		
<i>n</i> -Bu	$\text{OH}_2$	400		
Bz	$\text{OH}_2$	334		
Np	$\text{OH}_2$	307		
$\text{CH}_2\text{SiMe}_3$	$\text{OH}_2$	270		
$^{12}\text{C}^{14}\text{N}$	$^{12}\text{C}^{14}\text{N}$	379	493	2138
$^{13}\text{C}^{14}\text{N}$	$^{13}\text{C}^{14}\text{N}$	366	482	2088
$^{12}\text{C}^{15}\text{N}$	$^{12}\text{C}^{15}\text{N}$	377	492	2100
$^{13}\text{C}^{15}\text{N}$	$^{13}\text{C}^{15}\text{N}$	363	481	2057

**Electrochemistry of  $[\text{Co}(\text{bpb})\text{R}(\text{L})]$ .** The formal potentials for  $[\text{Co}(\text{bpb})\text{R}(\text{L})]$  complexes were determined by cyclic voltammetry and are listed in Table 1. The cyclic voltammograms for  $[\text{Co}(\text{bpb})\text{R}(\text{OH}_2)]$  (R =  $\text{CH}_3$ ,  $\text{C}_2\text{H}_5$ ,  $\text{CH}_2\text{SiMe}_3$ ) show reversible oxidation couples and irreversible reduction waves. On the basis of the EPR evidence described earlier, the oxidation couples are attributable to the metal-centered Co(III/IV) oxidation. Similar  $E^\circ[\text{Co}(\text{III/IV})]$  values were found for cobalt(III) alkyls of Schiff bases.<sup>15</sup> The  $E^\circ[\text{Co}(\text{III/IV})]$  values for  $[\text{Co}(\text{bpb})\text{R}(\text{OH}_2)]$  show a small dependence on the R group and roughly decrease in the order  $\text{CH}_3 \sim \text{CH}_2\text{SiMe}_3 > \text{C}_2\text{H}_5 > i\text{-Pr}$ . The oxidations of  $[\text{Co}(\text{bpb})\text{CH}_3(\text{PMe}_3)]$  and  $[\text{Co}(\text{bpb})(i\text{-Pr})(\text{OH}_2)]$  are irreversible presumably because such Co(IV) species generated are unstable with respect to Co–C scission on the cyclic voltammetric time scale.

**Raman Spectroscopy.  $[\text{Co}(\text{bpb})\text{R}(\text{L})]$ .** The solid-state FT-Raman data for  $[\text{Co}(\text{bpb})\text{X}(\text{L})]$  are summarized in Table 2. Figure 3 shows the Raman spectra obtained for  $[\text{Co}(\text{bpb})\text{R}(\text{L})]$ .

- (13) (a) Abley, P.; Dockal, E. R.; Halpern, J. *J. Am. Chem. Soc.* **1972**, *94*, 659. (b) Halpern, J.; Chan, M. S.; Hanson, J.; Roche, T. S.; Topich, J. A. *J. Am. Chem. Soc.* **1975**, *97*, 1606. (c) Topich, J. A.; Halpern, J. *Inorg. Chem.* **1979**, *18*, 1339.
- (14) Anson, F. C.; Collins, T. J.; Coots, R. J.; Gipson, S. L.; Richmond, T. G. *J. Am. Chem. Soc.* **1984**, *106*, 5037.
- (15) Levitin, I.; Sigán, A. L.; Vol'pin, M. E. *J. Chem. Soc., Chem. Commun.* **1975**, 469.

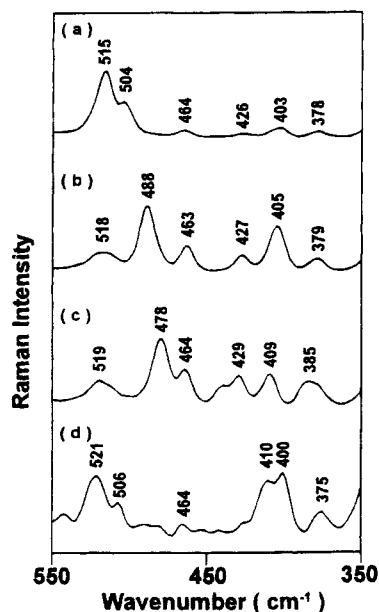


**Figure 3.** FT-Raman spectra of  $[\text{Co}(\text{bpb})\text{R}(\text{OH}_2)]$  in the solid state:  $\text{R} = \text{CH}_3$  (a),  $\text{C}_2\text{H}_5$  (b),  $i\text{-Pr}$  (c),  $n\text{-Bu}$  (d).

$(\text{OH}_2)_2$  in the solid state. The intense line for  $[\text{Co}(\text{bpb})\text{CH}_3(\text{OH}_2)]$  at  $515\text{ cm}^{-1}$ , which shifts to  $483\text{ cm}^{-1}$  upon deuteration of the axial methyl group, is confidently assigned to the Raman-active  $\text{Co}-\text{CH}_3$  stretching mode. The observed isotopic shift of  $32\text{ cm}^{-1}$  is in close agreement with the theoretical value of  $36\text{ cm}^{-1}$ . Similar stretching frequencies and isotopic shifts have been observed for  $[\text{Co}(\text{DH})_2\text{CH}_3]$  ( $510\text{ cm}^{-1}$ ) and methylcobalamin ( $500\text{ cm}^{-1}$ ).<sup>5</sup> Another isotopically sensitive line at  $403\text{ cm}^{-1}$  for  $[\text{Co}(\text{bpb})\text{CH}_3(\text{OH}_2)]$ , which is absent in the  $[\text{Co}(\text{bpb})(\text{OH}_2)]$  spectrum and downshifts to  $397\text{ cm}^{-1}$  upon deuteration, is assigned to the  $\text{C}-\text{Co}-\text{N}$  deformation mode, on the basis of the previous assignment for the cobaloxime analog.<sup>5</sup> Unlike the case of the cobaloxime system, the Raman spectrum for  $[\text{Co}(\text{bpb})\text{CH}_3(\text{OH}_2)]$  in methanol solution is essentially identical to that found in the solid state. The  $\text{Co}-\text{CH}_3$  stretching modes for the adducts  $[\text{Co}(\text{bpb})\text{CH}_3(\text{B})]$  ( $\text{B} = \text{PMe}_3$ ,  $t\text{-Bupy}$ ) are found at lower frequencies ( $500$  and  $511\text{ cm}^{-1}$ , respectively) but are considerably more intense (by ca. 10-fold) than that for  $[\text{Co}(\text{bpb})\text{CH}_3(\text{OH}_2)]$ . These results are consistent with those reported earlier for the methylcobaloxime analogs.<sup>5</sup>

The Raman spectrum for the ethyl compound  $[\text{Co}(\text{bpb})\text{C}_2\text{H}_5(\text{OH}_2)]$  (Figure 3b) shows a weak line at  $488\text{ cm}^{-1}$  which downshifts to  $449\text{ cm}^{-1}$  on deuteration of the axial ethyl ligand and is assigned to the  $\text{Co}-\text{C}$  stretching mode. A similar frequency and isotopic shift were found for ethylcobalamin, which are also of lower intensity compared to those for methylcobalamin.<sup>16</sup> The lower intensity of  $\nu(\text{Co}-\text{C})$  for the ethyl relative to the methyl counterpart can be explained in terms of coupling of the  $\text{Co}-\text{C}$  stretching mode with the  $\text{Co}-\text{C}-\text{C}'$  bending mode.

In an attempt to elucidate the influence of steric bulk of the alkyl ligand on the  $\text{Co}-\text{C}$  bond, we also studied  $\text{Co}(\text{bpb})$  complexes of heavier alkyl groups, viz. isopropyl,  $n$ -butyl, benzyl, neopentyl, and (trimethylsilyl)methyl, which might serve as models for the adenosyl group in coenzyme  $\text{B}_{12}$ . The determination of the  $\text{Co}-\text{C}$  stretch for bulky alkyls such as benzyl and neopentyl may provide clues for identification of  $\nu(\text{Co}-\text{C})$  for  $\text{B}_{12}$  coenzymes given the comparable steric bulks of neopentyl and adenosyl. As expected, the heavier the axial

alkyl group, the lower the frequency and intensity of the observed  $\text{Co}-\text{C}$  stretching mode. The  $\text{Co}-\text{C}$  stretching frequencies for  $i\text{-Pr}$ ,  $n\text{-Bu}$ ,  $\text{Bz}$ ,  $\text{Np}$ , and  $\text{CH}_2\text{SiMe}_3$  were determined to be respectively  $478$ ,  $400$ ,  $334$ ,  $307$ , and  $270\text{ cm}^{-1}$ . The assignments for  $\text{Co}-\text{C}$  stretches for the isopropyl and benzyl complexes have been confirmed by isotopic labeling.

**$[\text{Co}(\text{bpb})\text{CH}_3]^+$ .** Despite several attempts, we have not been able to obtain good-quality solid samples of  $[\text{Co}(\text{bpb})\text{CH}_3]^+$  for Raman study. The course of oxidation of  $[\text{Co}(\text{bpb})\text{CH}_3(\text{OH}_2)]$  and  $[\text{Co}(\text{bpb})\text{CD}_3(\text{OH}_2)]$  by  $(\text{NH}_3)_2[\text{Ce}(\text{NO}_3)_6]$  in methanol has been monitored by Raman spectroscopy. Upon addition of an equimolar amount of  $\text{Ce}(\text{IV})$  to  $[\text{Co}(\text{bpb})\text{CH}_3(\text{OH}_2)]$ , dramatic changes were observed in the Raman spectra. However, all peaks in the Raman spectra in the  $1700\text{--}200\text{ cm}^{-1}$  regions for  $[\text{Co}(\text{bpb})\text{CH}_3]^+$  and  $[\text{Co}(\text{bpb})\text{CD}_3]^+$  correspond to each other (within  $\pm 2\text{ cm}^{-1}$ ), except the modes associated with the  $\text{CH}_3$  and  $\text{CD}_3$  moieties, which are shifted significantly. It can be concluded that the  $\text{Co}-\text{CH}_3$  and  $\text{Co}-\text{CD}_3$  moieties in the above  $\text{Co}(\text{IV})$  compounds remain intact during oxidation, on the basis of the following evidence. First, the modes at  $517$  and  $404\text{ cm}^{-1}$  assignable to the  $\text{Co}-\text{C}$  stretching and  $\text{C}-\text{Co}-\text{N}$  deformation modes for  $[\text{Co}(\text{bpb})\text{CH}_3(\text{OH}_2)]$ , respectively, disappear on oxidation and the corresponding new lines are found at  $493$  and  $412\text{ cm}^{-1}$  for  $[\text{Co}(\text{bpb})\text{CH}_3]^+$ . A similar spectral change has been observed for the oxidation of  $[\text{Co}(\text{bpb})\text{CD}_3(\text{OH}_2)]$ , in which the corresponding modes at  $485$  and  $397\text{ cm}^{-1}$  shift to  $467$  and  $406\text{ cm}^{-1}$ , respectively. On the basis of the observed isotopic shift ( $26\text{ cm}^{-1}$ ), the line at  $493\text{ cm}^{-1}$  is assigned to the  $\text{Co}-\text{C}$  stretching mode for  $[\text{Co}(\text{bpb})\text{CH}_3]^+$ . Second, the intense band at  $1150\text{ cm}^{-1}$  for  $[\text{Co}(\text{bpb})\text{CH}_3]^+$  assignable to the symmetric deformation ( $\delta_s$ ) mode of the axial  $\text{CH}_3$  group was observed at  $882\text{ cm}^{-1}$  for  $[\text{Co}(\text{bpb})\text{CD}_3]^+$ . This isotopic shift ratio ( $0.767$ ) is in excellent agreement with the calculated value ( $0.769$ ).<sup>17</sup> Third, the bands at  $2881$  and  $2107\text{ cm}^{-1}$  assignable to the symmetric  $\text{C}-\text{H}$  stretching modes ( $\nu_s$ ) for  $[\text{Co}(\text{bpb})\text{CH}_3(\text{OH}_2)]$  and  $[\text{Co}(\text{bpb})\text{CD}_3(\text{OH}_2)]$ , respectively, were found to shift to ca.  $2893$  and  $2116\text{ cm}^{-1}$  for the  $\text{Co}(\text{IV})$  counterparts. Again, the observed isotopic shift ratio of  $0.731$  for both the  $\text{Co}(\text{III})$  and  $\text{Co}(\text{IV})$  complexes agrees well with the theoretical value of  $0.715$ .<sup>18</sup> In comparison, for the cobaloxime analogs the isotopic shift ratios have been found in the range  $0.759\text{--}0.765$  for  $\delta_s$  and at  $0.727$  for  $\nu_s$ .<sup>5</sup>

**$[n\text{-Bu}_4\text{N}][\text{Co}(\text{bpb})(\text{CN})_2]$ .** The  $\nu(\text{Co}-\text{C})$  and  $\delta(\text{Co}-\text{C}-\text{N})$  modes for  $[\text{Co}(\text{bpb})(\text{CN})_2]^-$  have been unambiguously assigned by selective isotopic substitution of the carbon and nitrogen of the axial cyanide by  $^{13}\text{C}$  and  $^{15}\text{N}$ . As expected, the  $\text{Co}-\text{C}$  stretching and bending modes were found to follow a "zig-zag" pattern. The former mode decreases from  $493$  to  $482\text{ cm}^{-1}$  on  $^{13}\text{C}^{14}\text{N}$  substitution for  $^{12}\text{C}^{14}\text{N}$ , then increases back to  $492\text{ cm}^{-1}$  on  $^{12}\text{C}^{15}\text{N}$  substitution, and finally decreases to  $481\text{ cm}^{-1}$  on  $^{13}\text{C}^{15}\text{N}$  substitution. The bending mode exhibits a similar decrease-increase-decrease pattern, appearing at  $377$ ,  $366$ ,  $377$ , and  $363\text{ cm}^{-1}$  for the  $^{12}\text{C}^{14}\text{N}$ ,  $^{13}\text{C}^{14}\text{N}$ ,  $^{12}\text{C}^{15}\text{N}$ , and  $^{13}\text{C}^{15}\text{N}$  labeled derivatives, respectively. Similar stretching and bending frequencies, as well as isotopic shift pattern, were also observed for the cyanocobalamin.<sup>14</sup> But unlike the  $\text{B}_{12}$  case, where the asymmetric corrin ring causes splitting of the  $\text{Co}-\text{C}$  vibrational modes,<sup>16</sup> there is no splitting found in the  $[\text{Co}(\text{bpb})(\text{CN})_2]^-$  system.

**$[\text{Co}(\text{por})\text{R}]$ .** The solid-state FT-Raman spectral data for  $[\text{Co}(\text{por})\text{CH}_3]$  are collected in Table 3. The isotopically sensitive

(17) (a) Krimm, S. *J. Chem. Phys.* **1960**, *32*, 1780. (b) Bakke, A. M. *J. Mol. Spectrosc.* **1972**, *41*, 1.

(18) Ervin, A. M.; Shupack, S. I.; Byler, D. M. *Spectrosc. Lett.* **1984**, *17*, 603.

**Table 3.** Co–C Vibrational Frequencies (cm<sup>-1</sup>) for [Co(por)R] in the Solid State

por	R	$\nu(\text{Co}-\text{C})$	por	R	$\nu(\text{Co}-\text{C})$
TPP	CH <sub>3</sub>	503	OEP	CD <sub>3</sub>	473
TPP	CD <sub>3</sub>	475	TMP	CH <sub>3</sub>	459
OEP	CH <sub>3</sub>	500	TMP	CD <sub>3</sub>	429

lines at 500, 503, and 459 cm<sup>-1</sup>, which shift to 473, 477, and 429 cm<sup>-1</sup> on deuteration of the axial methyl group, are confidently assigned to the Co–C vibrational modes for respectively [Co(OEP)CH<sub>3</sub>], [Co(TPP)CH<sub>3</sub>], and [Co(TMP)CH<sub>3</sub>]. It should be noted the  $\nu(\text{Co}-\text{C})$  for [Co(TPP)CH<sub>3</sub>] is not significantly different from that for the more electron-rich [Co(OEP)CH<sub>3</sub>]. However a remarkable downshift (41 cm<sup>-1</sup>) in  $\nu(\text{Co}-\text{C})$  was observed in comparing the sterically encumbered TMP complex with the TPP counterpart. The intensity of Co–C stretching frequency for [Co(por)CH<sub>3</sub>] is significantly lower than that for the cobalamin analog possibly because the latter is more polarizable in response to bond distortion. In addition, the absence of an axial base in the 5-coordinate [Co(por)CH<sub>3</sub>] also contributes to the low intensity of the Co–C stretch.

## Discussion

**Co(IV) Alkyls.** Organometallic complexes of Co(IV) are rare. The only structurally characterized Co(IV)  $\sigma$ -alkyl is the homoleptic 1-norbornyl complex.<sup>19</sup> *N*-deprotonated amido ligands are strong  $\sigma$  donors and thus are capable of stabilizing transition metals in high oxidation states.<sup>20</sup> Electrochemical data for [Co(bpb)R(OH<sub>2</sub>)] suggest that the Co(IV) alkyls [Co(bpb)R]<sup>+</sup> are reasonably stable and should be chemically accessible. Indeed, [Co(bpb)CH<sub>3</sub>]<sup>+</sup> could be isolated from oxidation of [Co(bpb)CH<sub>3</sub>(OH<sub>2</sub>)] at room temperature as a stable solid. [Co(bpb)CH<sub>3</sub>]<sup>+</sup> is more reactive than the Co(III) congener toward Co–C cleavage both thermally and photochemically. It is tempting to assume that the Co–C bond in [Co(bpb)R(OH<sub>2</sub>)] is weakened on oxidation. In fact, oxidation-induced Co–C bond cleavage/migration is well documented for organocobalt(III) compounds. Chemical or electrochemical oxidation of [Co(por)R] initially gives [Co(por)R]<sup>+</sup> that subsequently undergoes R migration from Co to the porphyrin N to give the *N*-substituted [N-RporCo]<sup>+</sup> species.<sup>21</sup> Electrochemical oxidation of organocobalt(III) complexes of Schiff bases and dimethylglyoxime gave reactive Co(IV) alkyls, which are only stable at low temperature.<sup>13,15</sup> It seems reasonable that Co(IV)–C bond is weaker than the Co(III)–C analog. This is indeed supported by our Raman evidence that oxidation of [Co(bpb)CH<sub>3</sub>(OH<sub>2</sub>)] resulted in a downshift of  $\nu(\text{Co}-\text{C})$  by 24 cm<sup>-1</sup>. Assuming that the Co–C bonds in both [Co(bpb)CH<sub>3</sub>(OH<sub>2</sub>)] and [Co(bpb)CH<sub>3</sub>]<sup>+</sup> follow the Morse potential curve relationship<sup>22</sup>

$$U_{(r)} = D_e \{1 - \exp[-a(r - r_e)]\}^2$$

(where  $U_{(r)}$  = potential energy,  $D_e$  = bond energy, usually taken as the bond dissociation energy,  $r$  = bond length,  $r_e$  = bond length at equilibrium, and  $a$  = constant), then the force constant ( $k$ ) is equal to the second derivative of  $U_{(r)}$  at  $r = r_e$ , i.e.,  $k = 2D_e a^2$ . The following expression can be derived from the

conventional relationship between force constant ( $\kappa$ ) and vibrational frequency ( $\nu$ ):

$$\nu/\nu' = (\kappa/\kappa')^{1/2} = (D_e/D_e')^{1/2}$$

Hence the BDE ratio of Co(IV)–C to Co(III)–C is estimated to be (493/517)<sup>2</sup> or 0.909. Such a weakening of Co–C bond can be explained in terms of contraction of the Co d orbitals and reduction in d(Co)–p(C) overlap upon increasing the oxidation state of Co. Unfortunately, we have not been able to obtain structural data for comparison of the Co(IV)–C and Co(III)–C bond distances.

**Raman Spectroscopy of Co Alkyls.** Stable [Co(bpb)R(L)] complexes represent a new class of B<sub>12</sub> model compounds for Raman study because they are good Raman scatterers and bpb shows no prominent absorption bands in the region of interest (550–300 cm<sup>-1</sup>). Prior to this work, the assignment of the Co–C vibrational mode has been reported for only the methyl derivatives of cobaloxime and cobalamin.<sup>5</sup> Interestingly the Co–C stretches for methyl-B<sub>12</sub> and the model compounds studied thus far lie within a narrow range (from 500 for CH<sub>3</sub>–Cbl<sup>5a</sup> to 515 cm<sup>-1</sup> for [Co(bpb)CH<sub>3</sub>(OH<sub>2</sub>)] in the solid state). Unlike the case of the methylcobaloxime system, however, the Co–CH<sub>3</sub> vibration mode for the solid sample of [Co(bpb)CH<sub>3</sub>(OH<sub>2</sub>)] is essentially identical to that in solution. This is understandable, as bpb is a rigid planar ligand and is unlikely to be distorted from planarity by solvation. The crystal structure of [Co(bpb)Et(OH<sub>2</sub>)] shows that the bpb ligand is essentially planar and the Co atom is only slightly displaced above the N<sub>4</sub> plane.<sup>9</sup>

**Steric Effect.** One issue we wish to address is whether a ground-state steric effect such as the bulk of the 5'-deoxyadenosyl plays a role in triggering Co–C bond homolysis in B<sub>12</sub> coenzyme. Previous findings suggested that the primary influence of the bulk of the alkyl group on the model systems is the increase in Co–C distances and Co–C–C' angles.<sup>23</sup> In this work we found that the frequency as well as the intensity of the Co–C vibrational mode for [Co(bpb)R(OH<sub>2</sub>)] decreases as the mass of the axial alkyl increases. The decrease in Co–C stretching frequency from the methyl to the (trimethylsilyl)-methyl derivative may be due to the increase of mass of the alkyl group and/or decrease in Co–C bond strength. It is difficult to separate these two factors at this point. Furthermore, as pointed out previously, the differences in Co–C BDE are not necessarily concentrated in the differences in intrinsic Co–C "bond strength" in the ground state. The BDE differences (a) may be a product-state effect and/or (b) may be distributed throughout the whole molecule.<sup>5c</sup> However, earlier reports suggested that the Co–C BDE of Co(III) alkyls is very sensitive to steric effect of the alkyl ligand.<sup>4c,24</sup> The structure of neopentylcobaloxime revealed that the Co–C–C' is severely distorted and the Co–C bond is significantly longer than that for the methyl analog.<sup>23</sup>

To probe the influence of the steric effect of the equatorial macrocyclic ligand on the axial Co–C bond, the Raman spectra of methylcobalt(III) porphyrins were studied. It is clear that the steric bulk of the porphyrin macrocycle has a significant influence on the Co–C bond in the ground state. The Co–C vibrational frequency for the sterically encumbered [Co(TMP)CH<sub>3</sub>] is remarkably lower than that for Co(TPP)CH<sub>3</sub>. Apparently the axial Co–C bond in the former complex is weakened

(19) Bryne, E. K.; Theopold, K. H. *J. Am. Chem. Soc.* **1989**, *111*, 3887.

(20) For a review see: Collins, T. J. *Acc. Chem. Res.* **1994**, *27*, 279.

(21) (a) Kadish, K. M.; Han, B. C.; Endo, A. *Inorg. Chem.* **1991**, *30*, 4502. (b) Dolphin, D.; Halko, D. J.; Johnson, E. *Inorg. Chem.* **1981**, *20*, 4348. (c) Callot, H. J.; Cromer, R.; Louati, A.; Gross, M. *Nouv. J. Chim.* **1984**, *8*, 765. (d) Perree-Fauvet, M.; Gaudemer, A.; Boucely, P.; Devynck, J. J. *Organomet. Chem.* **1976**, *120*, 439.

(22) Nagai, K.; Kitagawa, T.; Horimoto, H. *J. Mol. Biol.* **1980**, *136*, 271.

(23) (a) Randaccio, L.; Bresciani-Pahor, N.; Toscano, P. J.; Marzilli, L. G. *J. Am. Chem. Soc.* **1981**, *103*, 6347. (b) Bresciani-Pahor, N.; Randaccio, L.; Toscano, P. J.; Marzilli, L. G. *J. Chem. Soc., Dalton Trans.* **1982**, 567.

(24) Halpern, J. *Acc. Chem. Res.* **1982**, *15*, 238.

by nonbonding repulsion with the ortho methyls of the meso phenyl rings. Such an interaction plays a key role in the mechanism of  $B_{12}$ -dependent reactions. It is believed that the steric interactions of apoenzyme with both the  $B_{12}$  coenzymes and the adenosyl group promotes the rate of Co–C bond homolysis.<sup>25</sup> The crystal structures of adenosyl- and cyanocobalamins reveal severe crowding around Co.<sup>26–28</sup> It was also suggested that the steric interaction of the axial ligand with the substituents of the enzyme contributes to (a) the formation of 5-coordinate biologically important Co(III) corrinoids and (b) the weakening of the Co–C bond in alkylcobalamins.<sup>29</sup> The FT-Raman data in this work support the latter suggestion, at least in the case of sterically encumbered  $[Co(TMP)CH_3]$ . This conclusion can be extrapolated to the alkyl Co(III) corrins, although the greater flexibility of the corrin ring as compared to porphyrin must be considered. It is not clear whether flexibility of the corrin ring will enable the  $B_{12}$  coenzymes to “absorb” the additional steric shock or to undergo further distortion in the corrin macrocycle. However, it seems reason-

able to speculate that the corrin ring may act synergistically with an increase of steric interaction and distortion in order to help the “lift-off” of the axial alkyl group. Evidence for such speculation comes from the following: (a) the weakening of Co–C bond by the steric bulk of the porphyrin observed in the Co porphyrin examples of this work; (b) the significant puckered conformations of the corrin ring observed in  $B_{12}$  derivatives; and (c) the increased rate of the Co–C cleavage upon binding to the enzyme.<sup>29</sup> Structural distortions of the corrin ring have been suggested earlier by Toraya et al. and others to be important in the  $B_{12}$  enzymatic processes.<sup>30i–k</sup>

**Summary.** The Co–C stretching frequencies for  $[Co(bpb)CH_3(OH_2)]$ ,  $[Co(bpb)(CN)_2]^-$ , and  $[Co(por)CH_3]$  have been unambiguously determined by FT-Raman spectroscopy. The  $\nu(Co-C)$  for methyl- $B_{12}$  and the model compounds were found to lie within a narrow range (from 515 to 500  $cm^{-1}$ ). We have for the first time identified the Co–C vibrational modes for the ethyl, isopropyl, *n*-butyl, benzyl, neopentyl, and trimethylsilyl complexes of Co(III). The frequency and intensity of the Co–C vibrational mode in  $[Co(bpb)CH_3(L)]$  are strongly affected by trans axial base L. Oxidation of  $[Co(bpb)CH_3(OH_2)]$  results in lowering of the Co–C stretching frequency from 517 to 493  $cm^{-1}$ , suggesting that the Co–C bond is weakened by oxidation. In the methylcobalt porphyrin system, we found that the steric bulk of the porphyrin macrocycle has a profound influence on the Co–C vibrational mode.

**Acknowledgment.** We thank The Hong Kong University of Science and Technology, The Hong Kong Research Grants Council, and The Royal Society of Chemistry, U.K., for support.

**Supporting Information Available:** Tables of  $^1H$  NMR and UV/vis spectral data for the newly prepared  $Co(bpb)R(L)$  complexes, the solution FT-Raman spectra of  $Co(bpb)R(OH_2)$  and  $[Co(bpb)R]^+$  ( $R = CH_3, CD_3$ ), and the solid-state FT-Raman spectra for the methylcobalt(III) porphyrins (5 pages). Ordering information is given on any current masthead page.

IC9505054

- (25) (a) Schrauer, G. N.; Stadlbauer, E. A. *Bioinorg. Chem.* **1974**, *3*, 353. (b) Stadlbauer, E. A.; Holland, R. J.; Lamm, F. P.; Schrauer, G. N. *Bioinorg. Chem.* **1974**, *4*, 67.
- (26) Lenhart, P. G. *Proc. R. Soc. London* **1968**, *A303*, 45.
- (27) Lenhart, P. G.; Hodgkin, D. C. *Nature* **1961**, *192*, 937.
- (28) Savage, H. F. J.; Lindley, P. F.; Finney, J. L.; Timmins, P. A. *Acta Crystallogr.* **1987**, *B43*, 296.
- (29) Rossi, M.; Glusker, J. P.; Randaccio, L.; Summers, M. F.; Toscano, P. J.; Marzilli, L. G. *J. Am. Chem. Soc.* **1985**, *107*, 1729.
- (30) (a) Ichikawa, M.; Toraya, T. *Biochim. Biophys. Acta* **1988**, *952*, 191. (b) Toraya, T.; Watanabe, N.; Ichikawa, M.; Matsumoto, T.; Ushio, K.; Kukui, S. *J. Biol. Chem.* **1987**, *262*, 8544. (c) Toraya, T.; Matsumoto, T.; Ichikawa, M.; Itoh, T.; Sugawara, T.; Mizuno, Y. *J. Biol. Chem.* **1986**, *261*, 9289. (d) Ushio, K.; Fukui, S.; Toraya, T. *Biochim. Biophys. Acta* **1984**, *788*, 318. (e) Toraya, T.; Ishida, A. *Biochemistry* **1988**, *27*, 7677. (f) Toraya, T.; Fukui, S. In *B<sub>12</sub>: Dolphin*, D., Ed.; Wiley: New York, 1982; Vol. 2, Chapter 9. (g) Toraya, T.; Fukui, S. *Adv. Chem. Ser.* **1980**, *191*, 139. (h) Toraya, T.; Abeles, R. H. *Arch. Biochem. Biophys.* **1980**, *203*, 174. (i) Zagalak, B.; Pawelkiewicz, J. J. *Acta Biochim. Pol.* **1964**, *11*, 49. (j) Pagano, T. G.; Marzilli, L. G. *Biochemistry* **1989**, *28*, 7213. (k) Babior, B. M.; Krouwer, J. S. *CRC Crit. Rev. Biochem.* **1979**, *6*, 35.